Influence of Field Strength and Flexibility on the Transient Electric Birefringence of Segmentally Flexible Macromolecules

ARTICLE *in* THE JOURNAL OF PHYSICAL CHEMISTRY B · JUNE 2002

Impact Factor: 3.3 · DOI: 10.1021/jp014613p

3 AUTHORS:

Horacio Pérez-Sánchez
Universidad Católica San Antonio de Murcia
75 PUBLICATIONS **238** CITATIONS
SEE PROFILE

José García de la Torre
University of Murcia
217 PUBLICATIONS **6,099** CITATIONS
SEE PROFILE

F. Guillermo Díaz Baños
University of Murcia
47 PUBLICATIONS **472** CITATIONS
SEE PROFILE

Influence of Field Strength and Flexibility on the Transient Electric Birefringence of Segmentally Flexible Macromolecules

H. E. Pérez Sánchez, J. García de la Torre, and F. G. Díaz Baños*

Departamento de Química Física, Universidad de Murcia, 30071 Murcia, Spain

Received: December 19, 2001; In Final Form: April 16, 2002

The influence of field strength and flexibility on the transient electric birefringence (TEB) of segmentally flexible macromolecules is studied using a trumbbell with induced and permanent dipoles as a model. According to TEB experiments, the birefringence reaches a steady state after the application of an electric field, a situation which is simulated using a Monte Carlo method. Once the field is removed, relaxation is studied by simulating the Brownian dynamics of the system. Special care has been taken in the statistical quality of the data and the procedure for multiexponential fitting of the decay profiles to obtain the amplitudes and relaxation times. The results are compared with different treatments with occasional agreement and disagreement. The range of applicability of the method proposed by Allison and Nambi (*Macromolecules* **1992**, *25*, 759) is discussed. We found that for bent molecules relaxation decay depends on the averaged conformation, flexibility, orientation mechanism, and field intensity. In addition, we show that TEB experiments could be sufficient to characterize the averaged angle of a segmentally flexible macromolecule and its dispersion, mainly if the information concerning amplitudes and faster relaxation times is used.

Introduction

Transient electric birefringence (TEB), which is based on the time-dependence behavior of a macromolecular solution under the influence of an electric field,[1−4] is well-known as an interesting source of information about macromolecules.

A good example is the quantitative characterization of the global geometry and flexibility of the simple nonhelical structural elements in RNA and DNA. Such knowledge is important for understanding both the biological role of these molecules and their participation in the formation of structures of a higher order.[5,6] For this purpose, TEB is able to give precise estimations of the rotational diffusion constants for relatively short nucleic acid helices (between 100 and 200 base pairs) with and without nonhelical central elements.[7,8]

In recent years, different approaches to the understanding of TEB results have been proposed in the bibliography, a brief summary of which is given below. In addition, we summarize some questions that we shall try to clarify in this work.

Analytical Theories. In *rigid body treatment*, hydrodynamic properties of rigid macromolecules can be calculated using well-developed theoretical and computational procedures, based on bead models.[9−13] In this treatment, for a rigid body, the reorientational dynamics involved in processes such as orientation and relaxation under an electric field can be characterized by a set of five rotational relaxation times[11,14] τ_k, $k = 1, ..., 5$. For semiflexible, wormlike macromolecules, Hagerman and Zimm[15] assumed that the longest relaxation time could be adequately calculated as the average of the longest of the five relaxation times obtained using the rigid-body-treatment for a sample of instantaneous conformations compatible with a certain degree of flexibility. The rigid-body hypothesis has been successful in the description of transient electric birefringence of DNA.[15,16]

In different treatments, Wegener[17−20] and Harvey, García de la Torre and co-workers[21−25] developed formalisms that describe the diffusivity of segmentally flexible macromolecules with two subunits. These treatments provide instantaneous values of the diffusion, which depend on the size and shape of the subunits, the way in which they are connected, and their orientation in the instantaneous conformation; however, the degree of flexibility of the joint does not enter in the treatment.

Roitman and Zimm[26] were able to develop a quasianalytical description of the dynamics of the semiflexible trumbbell model, in a simplified case where the hydrodynamic interaction between the three beads is neglected. Among other properties, these authors treated the decay of electric birefringence and for an induced dipole orienting mechanism.[27−28] To make the analytical theory possible, the study was restricted to the region where the Kerr law for steady birefringence is valid, which means to the decays from orientations produced by very weak fields.

***τ*-Ratio Approach.** Vacano and Hagerman proposed the "*τ*-ratio approach",[8] which has been applied, with certain interesting modifications, to different cases: global flexibility in the tertiary structure of RNA, taking $tRNA^{Phe}$ as a model;[29] conformational changes in the binding place S15 of ribosomal RNA 16S induced by protein and Mg^{2+};[30] determination of the angle between the acceptor and anticodon stems of a truncated mithocondrial tRNA;[31] and flexibility of single-stranded DNA, using gapped duplex helices to determine the persistence length of Poly(dT) and Poly(dA).[32]

The "*τ*-ratio approach" is based in the comparison of the longest relaxation times between one linear straight macromolecule and another with a hinge of nonhelical elements. The ratio between relaxation times is related with the bond angle by means of a Monte Carlo analysis, with the result being the angle presented by the structure with segmental flexibility. From a methodological point of view, it is based on the idea that the longest relaxation time is related with the global dimensions of the macromolecule. However, the method is not able to

* To whom correspondence should be addressed: E-mail: fgb@um.es.

10.1021/jp014613p CCC: $22.00
Published on Web 06/11/2002

differentiate between a certain fixed angle and an average angle of the same value, which is a result of the flexibility. An improved version of this procedure is the "phased τ ratio" used by Friederich et al.[29] In the paper by Mills et al.,[32] the amplitude analysis is also included.

Correlation Function Analysis of Brownian Dynamics Simulation *without* Electric Field (BDCF). In recent years, it has become common to simulate the Brownian dynamics of macromolecules in solution and their orientation when an electric field is applied, or their related relaxation when this electric field is removed. Two different approaches have been used. Allison and Nambi[33] studied the TEB of DNA, simulating Brownian trajectories without any orienting electric field and analyzing the simulated trajectories with suitable correlation functions. One of their aims was to approach the complex nature of polyion alignment in electric fields, comparing two orienting mechanisms: induced dipole and saturated induced dipole. Two correlation functions were proposed (one for each mechanism) while a low-field transient electric birefringence approximation is assumed. This method has been applied in different studies; for example, Zacharias and Hagerman[6] developed an interesting study of the influence of the static and dynamic bends in the transient electric birefringence of RNA.

Brownian Dynamics Simulation *with* Electric Field (BDEF). Our group[34−39] studied the changes produced in birefringence through a direct analysis of the simulated trajectories, including the presence of an orienting electric field. In a previous work,[40] we investigated the transient electric birefringence of segmentally flexible macromolecules in electric fields of arbitrary strength. In that paper, we studied the decay of the electric birefringence from the steady-state value to zero, when an orienting electric field applied to a segmentally flexible macromolecule is switched off. We specifically considered the simplest model, the trumbbell, with only two subunits (two arms joining three beads) and an equilibrium angle of 0°. Using Brownian dynamics as the predicting tool for the dynamics of the molecule we improved statistics to obtain data with a very good signal-to-noise ratio. We found that the induced and permanent dipoles behaved differently in the relaxation process, being possible to describe the first independently of the intensity of the field, whereas the second showed a dependence on the field strength. Moreover, the time spectrum showed no dependence on the type of dipole or the field intensity, and amplitudes appear to be essential in characterizing the relaxation of the molecule. According to our results, hydrodynamic interaction may be very important in describing the relaxation times of a molecule, although amplitudes are not affected by this refinement, which should be a very interesting advantage for the application and development of different simplified theories.

Some Unanswered Problems. The approaches and results summarized above represent very relevant improvements for the TEB technique. However, some questions remain unanswered and we shall point to some of these below.

It should be clarified whether the permanent dipole is equivalent to the saturated induced dipole. Allison and Nambi, when obtaining equation A9 in their paper[33] (page 706) for the saturated induced dipole, assumed that the induced dipole is saturated from even very low fields. On the other hand, Zacharias and Hagerman,[6] when reviewing the same paper, identify permanent with saturated induced dipole (pages 320 and 322).

It has been proposed that relaxation of birefringence of a permanent dipole (or saturated induced dipole) is identical to that of an induced dipole. Allison and Nambi did not see any significant differences between the molecules simulated with pure induced and those simulated with saturated induced dipoles for linear DNA.[33] This idea appears to be accepted by Zacharias and Hagerman,[6] because they chose the correlation function of the saturated induced dipole (page 6) when trying to simulate an induced dipole. On the other hand, Wegener[20] found that the relative amplitudes (not the time constants) of the decay of birefringence were dependent on the orientation mechanism, particularly for high curvature angles. It would be interesting to check whether the results from Wegener[20] and Allison and Nambi[33] are compatible. Furthermore, it would also be interesting to check whether the field intensity, the orientation mechanism, or other factors affect the relaxation times.

It would be important to know whether the correlation functions proposed by in Allison and Nambi[33] are applicable to flexible and nonlinear (bent) systems. Allison and Nambi obtained equation A6 (page 765 of ref 33) for DNA fragments much shorter than their persistence length (rather rigid DNA fragments). With this equation, they obtained the distribution function used in the correlation function of the induced dipole. Moreover, when obtaining A9 (page 706), certain assumptions were made which are strictly valid only for a rigid rod. In Table 1 (page 763), the results for induced and saturated induced dipoles are compared. The values are all very similar, but they refer to very rigid macromolecules. Only a slight difference appears for 367 bp and $P = 50$ nm, a case of higher flexibility. Zacharias and Hagerman[6] used the equations proposed by Allison and Nambi[33] to study models with different central bends up to 90°.

It is worth investigating whether a "low field" criterion can be defined. Allison and Nambi (page 765) say that at low field neither times nor amplitudes are sensitive to the orientation mechanism. According to Zacharias and Hagerman,[6] the absence of any dependence of the relaxation times and amplitudes on the intensity of the orienting field defines an operative "low field" criterion to compare the decay of nucleic acids helices obtained experimentally and by computer simulation. This idea assumes the independence of the results obtained with respect to the intensity of the field. However, according to our previous paper,[40] relaxation for an induced dipole could be the same for low and high fields, although, in the case of permanent dipole, could depend on the intensity of the field even for low fields. The interest of the "low field" criterion arises from the molecule's lack of deformation. This deformation after reaching steady state has been previously studied,[38] although its evolution with time and the possible relation with decay parameters have not received much attention.

It is not clear whether TEB measurements are enough to determine angles and their degree of dispersion. Vacano and Hagerman[8] studied molecules that show segmental flexibility as a consequence of helical segments being connected by different joints (bulges, loops, branches, etc.). These authors were able to quantify the apparent angles and, in certain situations, the dispersion associated to these angles. They used TEB and the τ-ratio method. The procedure did not take into account amplitudes, which appear to be essential for the understanding of TEB results.[40] Moreover, according to Allison and Nambi,[33] the amplitudes are sensitive both to the average and dispersion of the bond angle but not to the intensity of the field. On the other hand, Zacharias and Hagerman[6] mentioned that a clear distinction between stable and disperse curvatures cannot generally be made on the basis of TEB measurements, especially for molecules of 150 bp and above. The similar

behavior of both curvatures stems from the fact that the behavior in the final region of the decay is determined mainly by the averaged values of a chain, an observation that was made originally by Roitman and Zimm.[26−28] Whatever the case, the study presented shows that in certain circumstances (for example, apparent angles lower than ≈80° and short enough molecules) amplitudes could reveal differences between rigid and highly flexible molecules.

It would be interesting to determine what information can be extracted from the faster components of the decay. The τ-ratio procedure is not applicable to the fastest components of the decay curves of birefringence. However, these components could contribute up to 80% of the curve when the bond angle is close to 90°.[40−43] As a consequence, if we ignore the faster components of the decay, we could be losing critical information, both concerning the conformation and the dynamics. In their study, Zacharias and Hagerman[6] do not include a detailed analysis of the fastest decay, the reason given being that values are affected significantly by the length of the Brownian step and by the treatment of the data. On the other hand, in our previous study,[40] we observed that some problems associated with the analysis of the decay profile are diminished when the statistical quality of the data is improved.

Model and Methods

Model: Trumbbell. We consider a segmentally flexible macromolecule composed of two quasirigid subunits ("arms") joined by a semiflexible swivel and interacting with an electric field. The mechanical, hydrodynamic, and electrooptical description of the model is as described in earlier papers.[38,40] We simply remind the reader that the potential energy of a given configuration of the model has one term associated to the bending, which is defined by

$$\frac{V_{\text{int}}}{k_{\text{B}}T} = Q(\alpha - \alpha_0)^2 \tag{1}$$

where α_0 is the equilibrium value of the angle defined by the subunit axes ($\alpha_0 = 0$ for fully extended, straight conformation) and Q is the flexibility parameter, with $Q = 0$ for the completely flexible case and $Q \rightarrow \infty$ for the completely rigid one.

Brownian Dynamics Simulation. The Brownian dynamics simulation of segmentally flexible macromolecules has been used previously by our group.[44−48] We use a simulation procedure based on the algorithm of Ermak and McCammon,[49] with a modification proposed by Iniesta and García de la Torre.[50] Each step is taken twice in a predictor−corrector manner and the position of the beads after the time step is obtained from the previous position. When the hydrodynamic interaction (HI) between beads is included, we use the Rotne−Prager−Yamakawa modification of the Oseen tensor,[51−52] which corrects for the nonpointlike nature of the frictional elements and correctly describes the possibility of overlapping (of equal-sized beads).

Brownian Dynamics *with* Electric Field (BDEF). The interaction between the molecule and the field arises from permanent or induced dipoles. The corresponding potential energy is given by

$$\frac{V_{\text{elect}}}{k_{\text{B}}T} = -\sum_{i=1}^{2} (a_i \cos\theta_i + b_i \cos^2\theta_i) \tag{2}$$

where $\cos\theta_i = (\mathbf{E}\cdot\mathbf{u}_i)/E$ is the cosine of the angle between the electric field **E**, and the arm vector, $\mathbf{u}_i$. The electric parameters are $b_i = 0$ for a purely permanent dipole moment and $a_i = 0$ for a purely induced moment. In the case of permanent dipoles, we consider the head-to-tail case, which is the usual situation for permanent dipoles in linear macromolecules. In the permanent head-to-tail dipole, a_1 is positive and a_2 is negative. The field intensity or, more precisely, the strength of the molecule-field interaction is governed by the a and b values, with a proportional to E and b proportional to E^2.

In the present study, we exclusively look at the birefringence decay. Therefore, the field-on, birefringence-rise first part of the simulation, which has to be lengthy to make sure that the steady state is reached, is useless for our purposes. To save computing time, we start the simulation with a sample of molecules generated with the Monte Carlo procedure in the presence of a field. For the birefringence decay, we have used the Brownian dynamics algorithm, and individual trajectories are simulated for a large number of molecules. At any given time, t, $P_2(\cos\theta_i)$ is evaluated for each arm ($i = 1$ or 2), with P_2 being the Legendre polynomial of degree 2, defined by $P_2(\cos\theta_i) = (3\cos^2\theta_i - 1)/2$. For each molecule, birefringence is calculated following

$$\Delta n^*(t) = \frac{r_{12}(t)}{r_{12}(t) + r_{23}(t)} P_2(\cos\theta_1(t)) + \frac{r_{23}(t)}{r_{12}(t) + r_{23}(t)} P_2(\cos\theta_2(t)) \tag{3}$$

and, from their averages, the final value is obtained. The terms r_{12} and r_{23} are the arms lengths, and for practical purposes, we can take every pre-P_2 term to be equal to $^1/_2$. The duration of the decay is sufficiently long so that the final birefringence is zero (within statistical error).

A way of expressing the results is to normalize to the zero-time value $\Delta n(0)$, with $t = 0$ when the field is switched-off:

$$\Delta n^*(t) = \frac{\Delta n(t)}{\Delta n(0)} \tag{4}$$

Unless we say the opposite, we shall use the normalization given by eq 4.

For a more detailed description of the BDEF method, the reader is referred to our previous paper.[40]

In the same way that eq 4 gives a normalized value for birefringence, it is useful to use dimensionless variables and parameters in both the simulation procedure and the presentation of results. So, lengths and distances are expressed in dimensionless form by dividing them by the spring length, b; forces are divided by kT/b and time is normalized by multiplying by $kT/\zeta b^2$, where $\zeta = 6\pi\eta_0\sigma$, with η_0 being the solvent viscosity and σ the bead radius. An asterisk hereafter denotes all dimensionless quantities.

Correlation Function Analysis of Brownian Dynamics Simulation *without* Electric Field (BDCF). The calculation of different correlation functions allows different parameters to be obtained from Brownian dynamics of macromolecules (e.g., transport and friction coefficients). In this particular case, Allison and Nambi[33] propose correlation functions that characterize the rotational dynamics.

More specifically, we can define a unitary vector, **A,** fixed to a coordinate system that moves with the particle. If θ_{A} is the angle formed between two orientations of this vector separated by a time t, then we can define $\cos\theta_{\text{A}}(t) = \mathbf{A}(t)\cdot\mathbf{A}(0)$. The correlation functions which interest us are defined as $F(0,t) =$

$f[P_i(\cos\theta_A)]$, where P_i is the Legendre polynomial of degree i, $P_1[\cos\theta_A(t)] = \cos\theta_A(t)$ and P_2 is as defined above.

The function proposed by Allison and Nambi[33] for an induced dipole is

$$H_s(lt', mt') = \frac{1}{(N-1)^2}\sum_{ik} P_2[\cos(\mathbf{u}_i(mt')\cdot\mathbf{u}_k(lt'))] \quad (5)$$

For a saturated induced dipole, the same authors propose the following correlation function:

$$H_i(lt',mt') = \frac{1}{(N-1)^3}\sum_{ijk} P_1[\cos(\mathbf{u}_i(mt')\cdot\mathbf{u}_j(mt'))]P_2[\cos(\mathbf{u}_j(mt')\cdot\mathbf{u}_k(lt'))] \quad (6)$$

From now on, we shall name them as CF−IND and CF−SIND, respectively.

Birefringence Decay Functions and Fittings. The resulting time decay series can be fitted to a sum of exponentials:

$$\Delta n^*(t) = y(t) = a_1 e^{-t/\tau_1} + a_2 e^{-t/\tau_2} + ... \quad (7)$$

Because of normalization, the $y(t)$ functions decay from $y(0) = 1$ to $y(\infty) = 0$, so that, in this case, $a_1 + a_2 + ... = 1$.

The fitted relaxation times and amplitudes are indexed as (τ_1, a_1), (τ_2, a_2), ..., etc. We adopt the convention that τ_1 is the longest relaxation time. For the multiexponential fit, we have employed the commercial program Sigmaplot.[50]

Analytical Theories. As commented above, although a complete theory of the dynamics of segmentally flexible macromolecules cannot be worked out, some approximations or assumptions allow the theoretical description of certain particular aspects.

The *rigid body treatment* (RBT) is fully implemented in the computer program HYDRO[15] for structures of N spheres. The results presented below have been obtained using this program. The results of Wegener's treatment are displayed in Figure 1 of Zacharias and Hagerman's paper.[6] We have chosen the results for the structures that interest us.

Roitman and Zimm[26,27] (RZ) characterized the normalized birefringence, as

$$\frac{\Delta n(t)}{\Delta n(0)} = \sum_p a_p e^{-\lambda_p t^*} \quad (8)$$

t^* is the reduced time and a_p and λ_p are coefficients, whose values are tabulated by the authors for various degrees of flexibility. The summation is an infinite series, but a moderate number of terms (10 in the tables) supposedly suffice for convergence. The applicability of the Roitman−Zimm[26,27] theory should be restricted to low-field results. The parallelism between eq 7 and eq 8 is obvious.

Results and Discussion

We have studied the relaxation process of Δn for segmentally flexible macromolecules with different orienting mechanisms, paying attention to both the influence of the intensity of the orienting field and flexibility. Two different equilibrium angles, $\alpha_0 = 0°$ and 90°, have been used.

Trumbbells with $\alpha_0 = 0°$. The first part of our study is devoted to a comparison of the results of different treatments of the amplitudes and relaxation times obtained from TEB, using the trumbbell with $\alpha_0 = 0$ as a model. The fact that flexibility differs (Q ranges from 0, total flexibility, to 50, quasirigidity), leads to different averaged conformations. This is an extension of the study presented in our previous paper[40] and allows us to compare BDEF with BDCF and analytical methods for rigid (RBT) and flexible models (RZ).

In the BDEF, we have simulated the birefringence decay for two extreme cases of the field strength: very low and infinitely high. In experimental work, the study of birefringence dynamics at very high (saturating) fields is uncommon because of problems with instrumentation, sample alterations, or data interpretation. On the other hand, low field is quite usual in experiments. For our purposes, both extremes are very illustrative for the study of field strength effects.

In these simulations, the time step has always been $\Delta t^* = 5 \times 10^{-4}$, $\alpha_0 = 0°$, and the radii of the spheres, when HI is included, 0.5. To be certain that the molecules have had time enough to relax completely, the duration of each trajectory is given between 2 and 3 units of time. To obtain a good fitting, the number of molecules needs to be very high, the reason for which has been mentioned previously.[40] For BDEF, we found that four independent simulations of 1×10^6 molecules in the best conditions (no HI, very low flexibility, and high field) and four independent simulations of 4×10^6 for the worst conditions (HI, high flexibility, and low field) are reasonable choices.

Obviously, in the BDCF, one decay profile is obtained for each model and orientation mechanism. In these simulations, the time step has always been $\Delta t^* = 5 \times 10^{-4}$, $\alpha_0 = 0°$, and the radii of the spheres, when HI is included, 0.5. The interval of times used for the correlation analysis has been established between $t^* = 0$ and 2. To obtain good statistical quality in the least favorable cases, the simulations are grouped into four subsets of 200 simulations each. Every simulation has a length of 150 000 steps (or $t^* = 75$). For the rest of the cases, each of the four subsets is averaged over 50 simulations.

The resulting decay data (for BDEF or BDCF) were submitted to biexponential analysis, obtaining the amplitudes and relaxation constants. In most of the curves, a third exponential can be detected accurately, although we think it is more illustrative for our purposes to present these results in the same format. In addition, other authors have used biexponential fittings, and given the statistical quality of the data, these are the usual results from the experiments. Finally, we have the advantage that biexponential fitting is more robust than triexponential, and in the cases studied, any improvement provided by a third exponential is slight. Note that in the decay from very high fields obtained in BDEF, birefringence is initially saturated, so that $\Delta n^*(0) = 1$. In the rest of the cases, the values have been normalized to the value at $t = 0$. In BDCF, the values are normalized in such a way that $\Delta n^*(0) = 1$.

Calculations for rigid trumbbells with $\alpha = 0$, 60, and 90° have been performed according to rigid body and Wegener's treatments. The results for relaxation times are identical for both treatments, and amplitudes can be obtained from the second. We must mention that, for simplicity, in these calculations the length of the arms, b, has been taken to be 1, which is slightly shorter than that obtained in the Brownian dynamics simulation of a quasirigid spring, $\langle b^2\rangle^{1/2} = 1.02$.

All of the results mentioned above are presented in Table 1.

Trumbbells with $\alpha_0 = 90°$. Bearing in mind the objectives of this work, the study must be completed with a nonlinear (bent) model. Moreover, after checking Table 1, some interesting features are observed which suggest that an extensive study for a trumbbell, with an equilibrium angle $\alpha_0 = 90°$, should be

TABLE 1: Results for the Biexponential Fittings of the Decay Profiles of Birefringence Obtained with Brownian Dynamics Simulation with and without Electric Field[a]

Q		a_1	τ_1	τ_2
0.0 $\langle\alpha\rangle = \pi/2$	$a = 1$	0.796 ± 0.036	0.190 ± 0.005	0.065 ± 0.007
	$a = \infty$	0.668 ± 0.003	0.173 ± 0.001	0.053 ± 0.001
	CF−SIND	0.506 ± 0.010	0.186 ± 0.002	0.072 ± 0.001
	$b = 0.5$	0.289 ± 0.068	0.180 ± 0.014	0.077 ± 0.004
	$b = \infty$	0.316 ± 0.019	0.166 ± 0.004	0.076 ± 0.001
	CF−IND	0.275 ± 0.010	0.186 ± 0.003	0.078 ± 0.001
	RBT	0.200	0.190	0.073
	RZ	0.219	0.184	0.080
0.5 $\langle\alpha\rangle = \pi/3$	$a = 1$	0.925 ± 0.003	0.248 ± 0.001	0.035 ± 0.002
	$a = \infty$	0.703 ± 0.004	0.246 ± 0.001	0.041 ± 0.001
	CF−SIND	0.753 ± 0.003	0.251 ± 0.001	0.051 ± 0.001
	$b = 0.5$	0.684 ± 0.026	0.252 ± 0.007	0.055 ± 0.005
	$b = \infty$	0.698 ± 0.003	0.246 ± 0.001	0.042 ± 0.001
	CF−IND	0.695 ± 0.003	0.252 ± 0.001	0.054 ± 0.001
	RBT	0.880	0.260	0.040
	RZ	0.672	0.239	0.058
50 $\langle\alpha\rangle = 0$	$a = 1$	1.000 ± 0.002	0.346 ± 0.003	
	$a = \infty$	0.999 ± 0.003	0.344 ± 0.001	
	CF−SIND	0.998 ± 0.002	0.347 ± 0.001	
	$b = 0.5$	0.984 ± 0.006	0.352 ± 0.002	
	$b = \infty$	0.988 ± 0.004	0.348 ± 0.001	
	CF−IND	0.997 ± 0.001	0.347 ± 0.002	
	RBT	1.000	0.334	
	RZ	0.991	0.319	0.009

[a] $\alpha_0 = 0$. Simulations performed without hydrodynamic interaction. The average $\langle\alpha\rangle$ refers to the absence of field. Analytical results for rigid body treatment (RBT) and Roitman and Zimm (RZ) are also included. For the references and procedures used to obtain these data, see text.

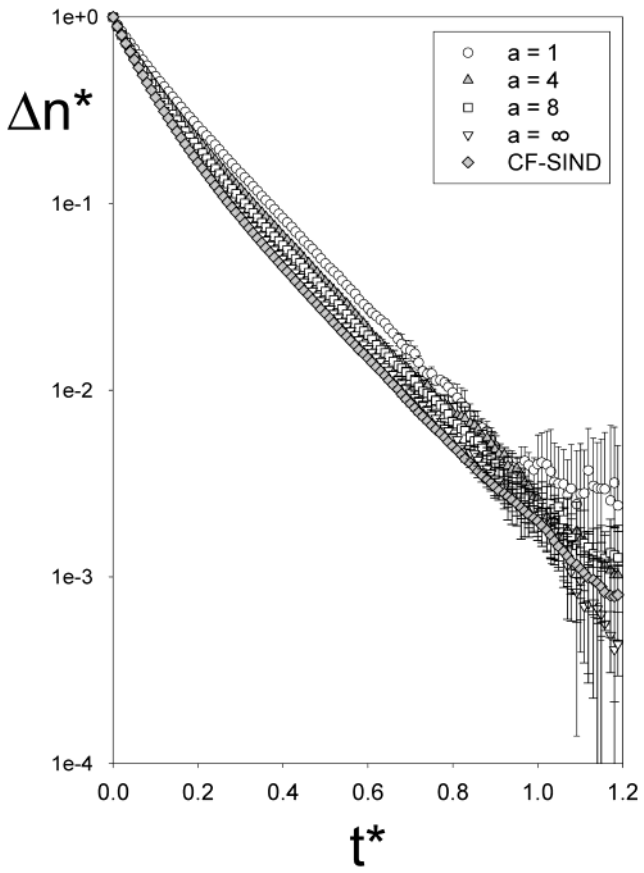

Figure 1. Birefringence decay profiles for different field intensities. Permanent dipole; $Q = 0.5$; no HI; $\alpha_0 = \pi/2$.

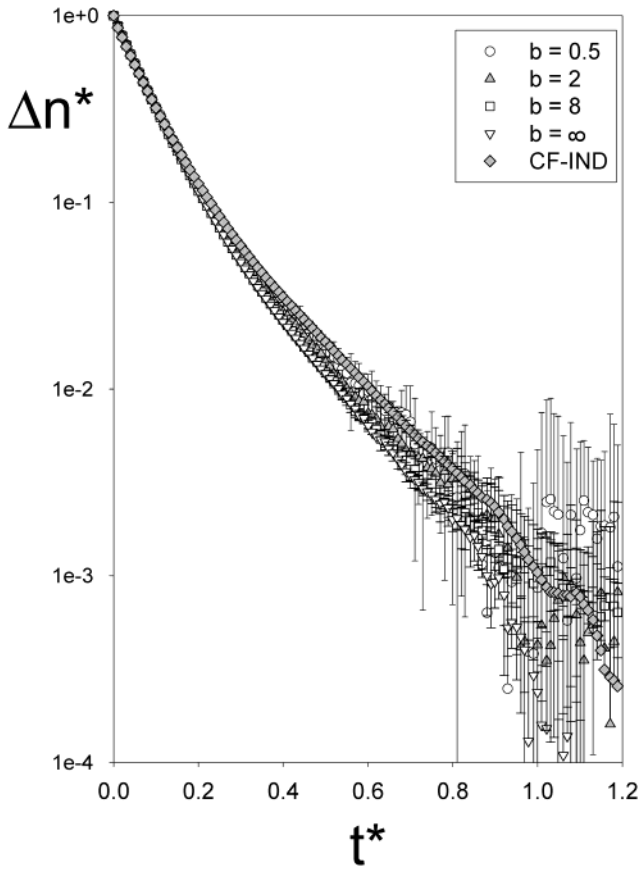

Figure 2. Birefringence decay profiles for different field intensities. Induced dipole; $Q = 0.5$; no HI; $\alpha_0 = \pi/2$.

developed. The choice of this model is interesting because different degrees of flexibility will give the same averaged angle, $\langle\alpha\rangle = 90°$, although a different dispersion of the angle will be associated to every value of Q.

In BDEF, we simulated the birefringence decay for different values of the field strength, from very low to infinitely high. This study was developed for models of different flexibilities and two orientation mechanisms, permanent head-to-tail and purely induced dipoles. In this way, we checked the influence of the different conditions in the decay profile. Simulations of BDCF were also performed for the two correlation functions, CF−IND and CF−SIND.

TABLE 2: Results of Fitting the Birefringence Decay Profile[a]

field	Q	a_1	τ_1	a_2	τ_2	a_3	τ_3
$a = 1$	0.0	0.801 ± 0.011	0.189 ± 0.003	0.199 ± 0.004	0.065 ± 0.002		
	0.1	0.778 ± 0.046	0.191 ± 0.004	0.222 ± 0.046	0.067 ± 0.012		
	0.5	0.769 ± 0.044	0.182 ± 0.005	0.212 ± 0.027	0.056 ± 0.009		
	2.5	0.725 ± 0.041	0.181 ± 0.007	0.275 ± 0.046	0.040 ± 0.006		
$a = 2$	0.0	0.715 ± 0.035	0.190 ± 0.003	0.261 ± 0.035	0.082 ± 0.007	0.025 ± 0.003	0.007 ± 0.002
	0.1	0.720 ± 0.020	0.187 ± 0.002	0.257 ± 0.018	0.076 ± 0.004	0.023 ± 0.002	0.006 ± 0.001
	0.5	0.625 ± 0.049	0.189 ± 0.005	0.344 ± 0.042	0.078 ± 0.008	0.032 ± 0.008	0.008 ± 0.003
	2.5	0.653 ± 0.008	0.181 ± 0.003	0.289 ± 0.012	0.050 ± 0.002	0.058 ± 0.008	0.007 ± 0.001
$a = 8$	0.0	0.583 ± 0.018	0.190 ± 0.003	0.384 ± 0.018	0.080 ± 0.002	0.033 ± 0.001	0.010 ± 0.001
	0.1	0.548 ± 0.010	0.191 ± 0.001	0.413 ± 0.008	0.080 ± 0.002	0.039 ± 0.002	0.012 ± 0.001
	0.5	0.505 ± 0.021	0.185 ± 0.003	0.452 ± 0.017	0.071 ± 0.003	0.043 ± 0.004	0.011 ± 0.001
	2.5	0.450 ± 0.005	0.180 ± 0.001	0.474 ± 0.002	0.045 ± 0.001	0.077 ± 0.006	0.008 ± 0.001
$a = \infty$	0.0	0.523 ± 0.016	0.188 ± 0.002	0.409 ± 0.011	0.080 ± 0.003	0.068 ± 0.005	0.016 ± 0.001
	0.1	0.508 ± 0.028	0.187 ± 0.004	0.430 ± 0.024	0.076 ± 0.004	0.062 ± 0.007	0.015 ± 0.001
	0.5	0.411 ± 0.038	0.187 ± 0.007	0.502 ± 0.019	0.074 ± 0.005	0.087 ± 0.020	0.020 ± 0.003
	2.5	0.297 ± 0.009	0.182 ± 0.003	0.384 ± 0.038	0.053 ± 0.002	0.319 ± 0.037	0.027 ± 0.001
CF−SIND	0.0	0.453 ± 0.018	0.193 ± 0.003	0.527 ± 0.015	0.079 ± 0.002	0.020 ± 0.003	0.013 ± 0.002
	0.1	0.428 ± 0.032	0.192 ± 0.002	0.545 ± 0.015	0.079 ± 0.005	0.027 ± 0.017	0.016 ± 0.007
	0.5	0.374 ± 0.020	0.185 ± 0.003	0.605 ± 0.012	0.073 ± 0.002	0.021 ± 0.008	0.012 ± 0.005
	2.5	0.270 ± 0.008	0.180 ± 0.003	0.695 ± 0.007	0.061 ± 0.001	0.035 ± 0.003	0.012 ± 0.001

[a] Permanent dipole (or saturated induced dipole for CF−SIND). No hydrodynamic interaction. $\alpha_0 = \pi/2$.

TABLE 3: Results of Fitting the Birefringence Decay Profile[a]

field	Q	a_1	τ_1	a_2	τ_2	a_3	τ_3
$b = 0.5$	0.0	0.271 ± 0.050	0.185 ± 0.013	0.730 ± 0.056	0.079 ± 0.003		
	0.1	0.262 ± 0.053	0.185 ± 0.016	0.738 ± 0.054	0.077 ± 0.003		
	0.5	0.191 ± 0.043	0.197 ± 0.018	0.809 ± 0.044	0.075 ± 0.002		
$b = 2$	0.0	0.211 ± 0.019	0.196 ± 0.005	0.772 ± 0.010	0.084 ± 0.002	0.016 ± 0.009	0.014 ± 0.008
	0.1	0.212 ± 0.013	0.190 ± 0.004	0.775 ± 0.010	0.082 ± 0.001	0.012 ± 0.003	0.011 ± 0.003
	0.5	0.178 ± 0.013	0.189 ± 0.004	0.808 ± 0.008	0.076 ± 0.001	0.014 ± 0.002	0.009 ± 0.002
$b = 8$	0.0	0.199 ± 0.023	0.197 ± 0.012	0.784 ± 0.021	0.086 ± 0.002	0.017 ± 0.004	0.010 ± 0.002
	0.1	0.185 ± 0.023	0.193 ± 0.008	0.800 ± 0.025	0.084 ± 0.001	0.015 ± 0.002	0.009 ± 0.001
	0.5	0.147 ± 0.008	0.193 ± 0.002	0.838 ± 0.008	0.077 ± 0.001	0.015 ± 0.001	0.008 ± 0.001
$b = \infty$	0.0	0.208 ± 0.009	0.188 ± 0.003	0.767 ± 0.009	0.085 ± 0.001	0.025 ± 0.003	0.013 ± 0.002
	0.1	0.196 ± 0.009	0.187 ± 0.003	0.780 ± 0.010	0.083 ± 0.001	0.024 ± 0.003	0.013 ± 0.002
	0.5	0.157 ± 0.006	0.184 ± 0.003	0.823 ± 0.007	0.077 ± 0.001	0.019 ± 0.003	0.014 ± 0.002
CF−IND	0.0	0.247 ± 0.014	0.192 ± 0.004	0.744 ± 0.012	0.081 ± 0.001	0.009 ± 0.002	0.009 ± 0.002
	0.1	0.226 ± 0.013	0.194 ± 0.004	0.764 ± 0.011	0.080 ± 0.001	0.010 ± 0.002	0.010 ± 0.002
	0.5	0.199 ± 0.014	0.190 ± 0.006	0.792 ± 0.013	0.076 ± 0.001	0.010 ± 0.001	0.008 ± 0.002

[a] Induced dipole. No hydrodynamic interaction. $\alpha_0 = \pi/2$.

In BDEF simulations, except for the value of the equilibrium angle, $\alpha_0 = 90°$, the rest of the conditions are the same as in the trumbbell with $\alpha_0 = 0°$ (only that no hydrodynamic interaction simulations were performed). Exactly the same can be said about BDCF. Figures 1 and 2 show examples of the decay profiles obtained.

After each simulation for BDEF or BDCF, the resulting decay profiles were submitted to multiexponential analysis as described above, providing amplitudes and relaxation constants. In most of the simulations, three exponentials can be detected accurately. The only exceptions are the cases for very low field, in which the signal-to-noise ratio is not good enough with our simulation conditions to be able to reproduce accurately the third exponential. In addition, we have checked that in the cases studied differences between bi- and triexponential fittings can be important, a significant degree of improvement being obtained with the second ones. Indeed, when analyzing biexponential fitting, the conclusions about the detailed dependence of the relaxation time and amplitudes could be misleading, because they may be artifacts of the fitting procedure. Bearing these facts in mind and given the scope of this work, we have opted to present the results for triexponential fittings, except for $a = 1$ and $b = 1$ which have two exponentials (Tables 2 and 3).

In attempts to obtain relaxation times and amplitudes accurately, the induced dipole is an especially difficult case. The shape of the decay profile is such that the amplitude of the longest relaxation time is much smaller that the amplitude of the faster components. As a consequence the final straight region dominated by τ_1 appears after one or even two decades of the decay (depending on Q). This fact enlarges the difficulty of the fitting procedure, especially if the quality of the data is limited. We suggest that a direct comparison with experimental results should to take into account the comments made in these paragraphs.

The electric field has the effect of deforming the molecule, and this aspect has also been treated. Except for a totally rigid macromolecule, the central angle must be treated as an average. In all cases where $\alpha_0 = 90°$, $\langle\alpha\rangle = 90°$, but different flexibilities are associated with different angle dispersion in the absence of field. In fact, the cases we use are the following: $Q = 0$, $\sigma_\alpha \approx 39°$; $Q = 0.1$, $\sigma_\alpha \approx 38°$; $Q = 0.5$, $\sigma_\alpha \approx 34°$; and $Q = 2.5$, $\sigma_\alpha \approx 23°$, where σ_α is the standard deviation in the distribution of α. When an electric field is applied, the molecule suffers a certain deformation. This deformation is manifested in a change of $\langle\alpha\rangle$ which will vary depending on E, Q, and the orienting mechanism. After removing the field, $\langle\alpha\rangle$ returns to 90° following a certain time course. These processes affect the TEB decay profile. We have studied this aspect and an illustration is shown in Figure 3.

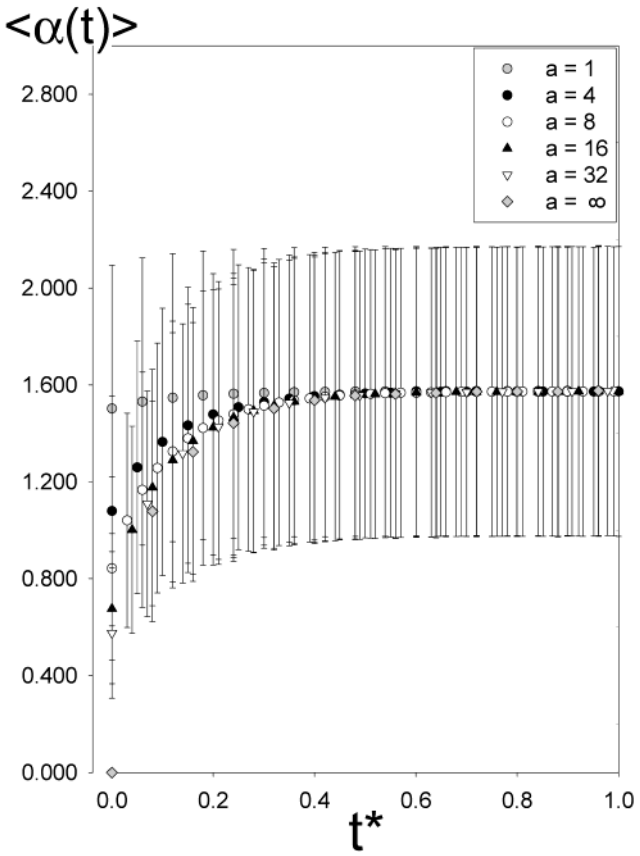

Figure 3. Evolution of central angle, α, with time. Permanent dipole; $Q = 0.5$; no HI.

Discussion of the Results

The two correlation functions are not identical for flexible or bent systems. The two correlation functions (for induced and saturated induced dipoles) do not always give the same decay profile. As can be seen in Table 1, when linearity of the averaged conformation is lost, both functions provide different decays. These differences appear in amplitudes and are bigger as the central angle, $\langle\alpha\rangle$, grows. Relaxation times are practically identical. This behavior is the same when hydrodynamic interaction is included (results not shown). We remind the reader that Allison and Nambi[33] developed their theory for short fragments of DNA, which can be approximated to straight and rigid molecules. Zacharias and Hagerman[6] assumed that both functions give the same results for any model.

When flexibility increases and linearity is lost the results from BDCF differ from those obtained by BDEF. When $\alpha_0 = 0$ and the molecule is rigid, all treatments give the same results for any field strength and any mechanism (see Table 1). However, when flexibility increases (averaged conformations are bent), some clear differences arise between permanent head-to-tail dipole (obtained by BDEF) and saturated induced dipole (obtained by BDCF and the corresponding CF−SIND correlation function). These differences can be observed in Table 1 (for $\alpha_0 = 0$) and also in Table 2 and Figure 1 (for $\alpha_0 = \pi/2$). For a given flexibility of the trumbbell, the results for the permanent dipole point to a dependence of the decay profiles on the intensity of the field. On the other hand, using BDCF and the CF−SIND function only a curve obtained for each value of Q, and this decay cannot be identified with any of the profiles obtained for permanent dipole. As a consequence, the saturated induced dipole should not be used to study permanent dipole systems. For the induced dipole, differences between both treatments are much smaller and almost negligible for lower fields (see Table 1). Indeed, because CF−IND was deduced for low fields, it is not surprising that, when the intensity of the field increases and $Q = 0$, the values of a_1 and τ_1 differ. BDEF and BDCF for the induced dipole are only comparable for low fields, and in these conditions, both treatments give very similar results, as is illustrated in Figure 2 for a model with $\alpha_0 = \pi/2$ and $Q = 0.5$. These comments can be extended when hydrodynamic interaction is included (results not shown).

Relaxation decays depend on the averaged conformation, flexibility, orientation mechanism and intensity of the field. This dependence is a very important source of information that can be exploited for characterizing amplitudes and relaxation times independently.

Amplitudes depend strongly on the mechanism of orientation. This is clearly observed when examining the results shown in Tables 1−3. Important differences appear in the amplitudes values, mainly when the averaged angle is $\langle\alpha\rangle = 90°$. Although, for permanent dipole, the amplitude associated with the longest relaxation time is the largest and can reach around 80%, this component is only around 25% for a model with the same flexibility and induced dipole.

Amplitudes depend on both the intensity of the field and the flexibility of the model. This is consistent with the results of Dieckman et al.,[54] who showed the influence of the electric field on the amplitudes. When working at low fields, it has been proposed[6] that amplitudes are sensitive to the average and dispersion of the angle but not to the field. According to our results for permanent dipoles (Table 2), a dependence on the field is observed even for the lowest intensity that can be simulated. For induced dipoles, the variation of a_1 with the field is very slight (Table 3) and so small that it would probably be undetectable in experiments. In addition, both orientation mechanisms show an important dependence on Q.

Relaxation times depend mainly on the internal angle (either fixed or averaged). This is the fundamental parameter that defines the global dimensions of the model (see Table 1). This conclusion was partially proposed by Diekmann et al.,[54] who suggested that the longest relaxation time is mainly influenced by the value of the averaged angle. According to Allison and Nambi,[33] all times reflect global rotational movements, and the fact that the relaxation times depend on flexibility for a lineal model like DNA is probably only due to the variation in the end-to-end distance. Moreover, according to Roitman and Zimm,[27] relaxation times are characteristic of a molecule and, as a consequence, do not depend on the method used to obtain them.

Indeed, in Table 1, it can be seen that the value of the longest relaxation time increases with Q. When total flexibility $Q = 0$, $\langle\alpha\rangle = \pi/2$, and as a consequence, the value of the longest relaxation time differs from the value when flexibility is intermediate ($Q = 0.5$ with $\langle\alpha\rangle = \pi/3$). When $Q = 50$, $\alpha_0 = 0 \approx \langle\alpha\rangle$, and τ_1 is that of a straight molecule. For any flexibility, when $\alpha_0 = \pi/2$, then $\langle\alpha\rangle = \pi/2$, and as a consequence, the value of the longest relaxation time is the same. Our results confirm that the longest relaxation time does not depend on the orienting mechanism. This is clearly shown when comparing both mechanisms in any case of Q (see Tables 2 and 3).

TEB relaxation times are the same as those involved in other hydrodynamic properties. This is the conclusion reached if we compare our results with those offered by the hydrodynamic theory for rigid models. The results are shown in Table 1, and differences are small. They support the idea that the relaxation times depend fundamentally on the angle (fixed or apparent).

On the other hand, TCR appears as a reasonable approximation when data quality is not critical.

Flexibility only slightly affects relaxation times when the averaged angle is the same. This conclusion is based on results shown in Tables 2 and 3. The dependence of τ_1 is almost negligible. Regarding the faster relaxation times, the dependence on Q is more important. For $a = 1$ and $b = 0.5$, only two exponentials are shown for the reasons given above, and this fact affects the value of τ_2. Indeed, after carefully analyzing our results, we believe that the differences from the rest of values for a and b are due to the type of fitting used. When three exponentials are used, the fastest relaxation time and its associated amplitude are very small, although significant and reproducible. The values which are higher for more flexible models show and a tendency to increase with the field.

A flexible molecule is deformed by an electric field of any intensity. Of course, the magnitude of that deformation is directly related to the orienting mechanism, intensity of the field and the degree of flexibility (Figure 3). For the permanent dipole in conjunction with the lowest field of our computational experiments, which corresponds to a value of $\Delta n(0)$ between 20 and 35 times smaller than the saturation value (depending on Q), the decay profile still depends on the intensity of the field for all values of Q studied. As can be expected, no relevant deformation is observed for the induced dipole for any intensity of the field or any degree of flexibility. The deformation of a macromolecule after reaching its steady state was studied in a previous work.[38]

On the other hand, the effect of deformation on the decay profile is small in most of the cases and less significant for slower components. In fact, as we have mentioned above, the dependence of the longest relaxation times with the field is nearly negligible, for both permanent head-to-tail and induced dipoles. The shortest times show a greater dependence (see Tables 2 and 3), which we think is a consequence of the deformation produced by the application of the electric field. In Figure 1, it can be seen that, for $t^* = 0.4$ in the decay profiles, the decay is nearly monoexponential and governed by the longest relaxation time; at the same time, in Figure 3, it can be seen that, for $t^* = 0.4$ and for all cases of flexibility, deformation is negligible. In principle, the deformation could be quantified as a function of the field by comparing the fastest components (preferentially amplitudes and relaxation times of triexponential fittings) for molecules with different degrees of flexibility. From a practical point of view, this would probably be very difficult because of the amount and quality of the data needed to obtain appropriate results.

According to our results, fixed and apparent angles can be distinguished using TEB. In our model, Q defines flexibility, and so, a direct relation can be established between dispersion of the central angle and amplitudes. For both orientation mechanisms, the decay profile depends on the intensity of the field and on Q, although the form of this dependence differs. Computational experiments allow us to ascertain the amplitude values as a function of Q and E. These results could be combined with laboratory experiments to determine Q and, as a consequence, the angle dispersion, a conclusion which might have a direct application in the design of TEB experiments.

Acknowledgment. This work has been funded by Grant BQU2000-0229 from Dirección General de Investigación Científica y Técnica (Ministerio de Educación y Cultura).

References and Notes

(1) Fredericq, E.; Houssier, C. *Electric Dichroism and Electric Birefringence*; Clarendon Press: Oxford, U.K., 1973.
(2) O'Konski, C. T., Ed. *Molecular Electrooptics, Part1- Theory and Methods*; Marcel Dekker: New York, 1976.
(3) Krause, S., Ed. *Molecular electrooptics*; Plenum Press: New York, 1981.
(4) Riande, E.; Saiz, E. *Dipole Moments and Birefringence of Polymers*; Prentice Hall: Englewood Cliffs, NJ, 1992.
(5) Hagerman, P. *Methods Enzymol.* **2000**, *317*, 440.
(6) Zacharias, M.; Hagerman, P. *Biophys. J.* **1997**, *73*, 318.
(7) Hagerman, P. *Curr. Opin. Struct. Biol.* **1996**, *6*, 643.
(8) Vacano, E.; Hagerman, P. J. *Biophys. J.* **1997**, *73*, 306.
(9) García de la Torre, J. *Eur. Biophys. J.* **1994**, *23*, 307.
(10) García de la Torre, J.; Bloomfield, V. A. *Biopolymers* **1977**, *16*, 1747.
(11) García de la Torre, J.; Bloomfield, V. *Quart. Rev. Biophys.* **1981**, *14*, 81.
(12) García de la Torre, J. Rotational diffusion coefficients. In *Molecular Electrooptics*; Krause, S., Ed.; Plenum Publishing Corporation: New York, 1981.
(13) García de la Torre, J.; Navarro, S.; López Martínez, M. C.; Díaz, F. G.; López Cascales, J. *Biophys. J.* **1994**, *67*, 530.
(14) Carrasco, B.; García de la Torre, J. *Biophys. J.* **1999**, *76*, 3044.
(15) Hagerman, P.; Zimm, B. H. *Biopolymers* **1981**, *20*, 1481.
(16) García Molina, J. J.; Lopez Martinez, M. C.; Garcia de la Torre, J. *Biopolymers* **1990**, *29*, 883.
(17) Wegener, R. M.; Dowben, R. M.; Koester, V. J. *J. Chem. Phys.* **1979**, *70*, 622.
(18) Wegener, R. M.; Dowben, R. M.; Koester, V. J. *J. Chem. Phys.* **1980**, *73*, 4086.
(19) Wegener, R. M. *J. Chem. Phys.* **1982**, *76*, 6425.
(20) Wegener, R. M. *J. Chem. Phys.* **1986**, *84*, 5989.
(21) Harvey, S. C. *J. Chem. Phys.* **1978**, *69*, 3426.
(22) Harvey, S. C.; Cheung, H. *Biopolymers* **1979**, *18*, 1081.
(23) Harvey, S. C.; Mellado, P.; García de la Torre, J. *J. Chem. Phys.* **1983**, *78*, 2081.
(24) García de la Torre, J.; Mellado, P.; Rodes, V. *Biopolymers* **1985**, *24*, 2145.
(25) Mellado, P.; Iniesta, A.; Díaz, F. G.; García de la Torre, J. *Biopolymers* **1988**, *27*, 1771.
(26) Roitman, D. G.; Zimm, B. H. *J. Chem. Phys.* **1984**, *81*, 6333.
(27) Roitman, D. G.; Zimm, B. H. *J. Chem. Phys.* **1984**, *81*, 6348.
(28) Roitman, D. G. *J. Chem. Phys.* **1984**, *81*, 6356.
(29) Friedrich, M. W.; Vacano, E.; Hagerman, P. *Biochemistry* **1998**, *95*, 3572.
(30) Orr, J.; Hagerman, P.; Williansom, J. *J. Mol. Biol.* **1998**, *275*, 453.
(31) Frazer-Abel, A.; Hagerman, P. *J. Mol. Biol.* **1999**, *285*, 581.
(32) Mills, J. B.; Vacano, E.; Hagerman, P. J. *J. Mol. Biol.* **1999**, *285*, 245.
(33) Allison, S. A.; Nambi, P. *Macromolecules* **1992**, *25*, 759.
(34) Pérez Belmonte, A.; López Martínez, M. C.; García de la Torre, J. *J. Phys. Chem.* **1991**, *95*, 952.
(35) Pérez Belmonte, A.; López Martínez, M. C.; García de la Torre, J. *J. Phys. Chem.* **1991**, *95*, 5661.
(36) Carrasco, B. *Tesis de Licenciatura*, Universidad de Murcia, 1995.
(37) Carrasco Gómez, B.; Pérez Belmonte, A.; López Martínez, M. C.; García de la Torre, J. *J. Phys. Chem.* **1996**, *100*, 9900.
(38) Carrasco, B.; Díaz, F. G.; López Martínez, M. C.; García de la Torre, J. *J. Phys. Chem. B* **1999**, *103*, 7822.
(39) Navarro, S.; López Martinez, M.; García de la Torre, J. *J. Polym. Sci. B: Polym. Phys.* **1997**, *35*, 689.
(40) Díaz, F. G.; Carrasco, B.; López Martinez, M.; García de la Torre, J. *J. Phys. Chem. B* **2000**, *104*, 12339.
(41) Friedrich, M. W.; Gast, F.; Vacano, E.; Hagerman, P. *Proc. Natl. Acad. Sci. U.S.A.* **1995**, *92*, 4803.
(42) Zacharias, M.; Hagerman, P. *J. Mol. Biol.* **1995**, *247*, 486.
(43) Zacharias, M.; Hagerman, P. *Proc. Natl. Acad. Sci. U.S.A.* **1995**, *92*, 6052.
(44) Díaz, F. G.; García de la Torre, J. *J. Phys. Chem.* **1988**, *88*, 7698.
(45) Díaz, F. G.; García de la Torre, J. *Macromolecules* **1994**, *27*, 5371.
(46) Díaz, F. G.; García de la Torre, J.; Freire, J. J. *Macromolecules* **1990**, *23*, 3114.
(47) Díaz, F. G.; Iniesta, A.; García de la Torre, J. *Biopolymers* **1990**, *29*, 547.
(48) Díaz, F. G.; López Cascales, J. J.; García de la Torre, J. *J. Biochem. Biophys. Methods* **1993**, *26*, 261.
(49) Ermak, D. L.; McCammon, J. A. *J. Chem. Phys.* **1978**, *69*, 1352.
(50) Iniesta, A.; Garcia de la Torre, J. *J. Chem. Phys.* **1990**, *92*, 2015.
(51) Rotne, J.; Prager, J. *J. Chem. Phys.* **1969**, *50*, 4831.
(52) Yamakawa, H. *J. Chem. Phys.* **1970**, *53*, 436.
(53) Sigmaplot for Windows, version 4.00; SPSS Inc.: Chicago, IL, 1997.
(54) Diekmann, S.; Hillen, W.; Morgeneyer, B.; Wells, R.; Porschke, D. *Biophys. Chem.* **1982**, *15*, 263.